METEOROLOGICAL APPLICATIONS
Meteorol. Appl. **23**: 438–447 (2016)
Published online in Wiley Online Library
(wileyonlinelibrary.com) DOI: 10.1002/met.1568

RMetS
Royal Meteorological Society

Vertical structure of summer clear-sky atmospheric boundary layer over the hinterland and southern margin of Taklamakan Desert

Minzhong Wang,[a,b,c,*] Hui Lu,[b,c] Hu Ming[d] and Jiantao Zhang[b,c]

[a] *Chinese Academy of Meteorological Sciences, Beijing, China*
[b] *Institute of Desert Meteorology, CMA (China Meteorological Administration), Urumqi, China*
[c] *Taklamakan Desert Atmospheric Environment Observation Experimental Station, Tazhong, China*
[d] *The Northwest Airline Management Bureau, CAAC, Xi'an, China*

ABSTRACT: The Urumqi Institute of Desert Meteorology of China Meteorological Administration carried out a scientific experiment to detect the clear-sky atmospheric boundary layer by using a wind-profiling radar and L-band radar sounding system in the hinterland and southern margin of the Taklamakan Desert in the summer of 2010 and 2011. Based on wind profile and radiosonde data collected from this experiment, this paper analyses the vertical structure features of the clear-sky daytime convective boundary layer and night-time stable boundary layer in the hinterland and southern margin of the desert, and compared the result with the boundary layer features in the Tibetan Plateau and the Dunhuang region in Gansu. The results show that: (1) the summer clear-sky convective boundary layers in the hinterland and southern margin of the Taklamakan Desert can develop thickly. The mixing layer can reach a maxiumum thickness of 3700 m, above which a significant entrainment layer exists with average thickness about 500 m. The maximum thickness of the convective boundary layer can exceed 4000 m. (2) A temperature inversion phenomenon is found to exist remarkably over the summer clear-sky nights in the hinterland and southern margin of the desert. The thickness of the night stable boundary layer is about 400–600 m, but the residual layer above it generally can reach a thickness of more than 3000 m. (3) An atmospheric boundary layer with supernormal thickness under the clear summer sky is a phenomenon of arid regions in Northwest China.

KEY WORDS Taklamakan Desert; deep convective boundary layer; entrainment layer; wind-profiling radar

Received 5 August 2015; Revised 22 December 2015; Accepted 23 January 2016

1. Introduction

The atmospheric boundary layer is where the interaction between the lower atmosphere and the Earth's surface is at its most intense and complex. It bridges the Earth and free atmosphere, being the channel for matter and energy exchange and closely connected with the formation and evolution of weather, climate and atmospheric environment (Zhang *et al.*, 2011). Boundary thickness is one of the most important physical parameters among the atmospheric boundary layer parameters. It decides directly the atmospheric environmental capacity of a region, and also strongly influences the evolution of clouds and convective process (Zhang, 2007). Earlier studies generally considered that the thickness of the convective boundary layer in the daytime was lower than 2000 m and the maximum thickness of a stable boundary layer in the night time was <400–500 m (Garratt, 1992). However, research during the past decade on the atmospheric boundary layer in specific geographical environments and extreme climatic backgrounds has transformed our understanding based on the earlier research (Raman *et al.*, 1990; Gamo *et al.*, 1994; Gamo, 1996; Zhang and Wang, 2008). Marsham *et al.* (2008) observed a convective boundary layer as thick as 5500 m in the Sahara desert with noticeable residual layer features. Takemi (1999) analysed the atmospheric boundary layer structure over the Hexi Corridor region of China by using convectional meteorological sounding data and found a presumed convective boundary layer with a thickness over 4000 m based on residual layer features. Zhang *et al.* (2007) conducted deeper research on the structure features of the atmospheric boundary layer and land surface processes in the arid region of Northwest China using observation data collected during the Dunhuang experiment, finding that the summer clear-sky convective boundary layer in Dunhuang could reach a thickness of 4000 m or more.

The Taklamakan Desert is the world's second largest flow desert and also is extremely sensitive to climate change in the arid region of Northwest China. This desert has a harsh natural environment with extremely dry climate and large range of drifting sand dunes. Compared with the other regions of the globe, its land surface processes and boundary layer structures are very unusual and have an important influence on the regional weather, climate and atmospheric circulation.

At present, research related to the atmospheric boundary layer in the Taklamakan Desert is concentrated mostly on near-surface meteorological observation experiments and analyses (He *et al.*, 2010a, 2010b; Wen *et al.*, 2010; Liu *et al.*, 2012; Yang *et al.*, 2013). He (2009) studied the land–air interaction and the near-surface air structure of the desert hinterland by virtue of an 80 m meteorological tower, approximately estimating the convective boundary layer in the summer desert to be about 3000 m. Xu *et al.* (2014), using the NCEP reanalysis data, studied the atmospheric boundary layer structure of the Taklamakan Desert and suggested that the thickness of the convective boundary layer can reach 3000–4000 m. However, all these research results need

* Correspondence: M. Z. Wang, Chinese Academy of Meteorological Sciences, 46 Zhongguancun South Street, Haidian District, Beijing, 100081, China. E-mail: yurenkeji@sina.com

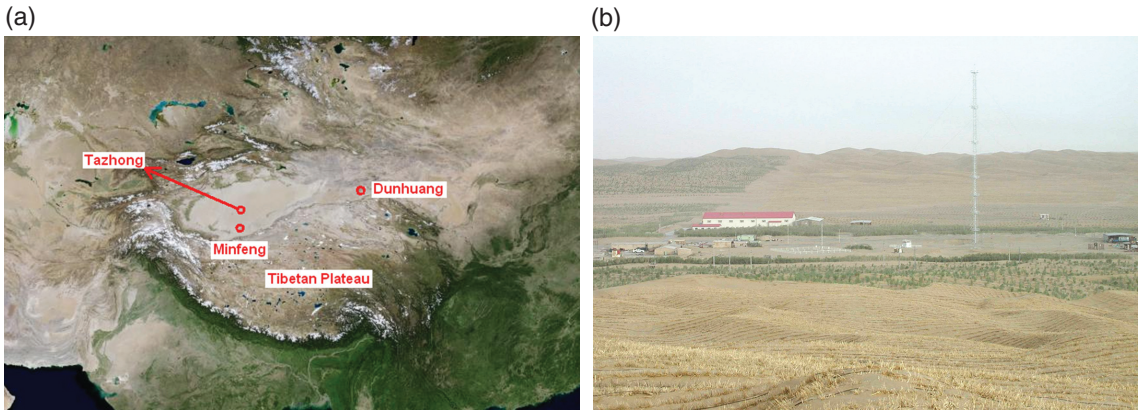

Figure 1. (a) Image showing the study area. (b) The atmosphere environment observation station in the Taklamakan Desert, Xinjiang autonomous area, China.

further observation and analysis for verification. In this study, a detection experiment was carried out on the summer clear-sky atmospheric boundary layer over the hinterland and southern margin of the Taklamakan Desert using a CFL-03 wind-profiling radar and an L-band radar sounding system. This paper analyses the vertical structures of the clear-sky daytime convective boundary layer and night time stable boundary layer, and compare them with boundary layer structures in the Tibetan Plateau and the Dunhuang region in Gansu province in order. Its aim is to enhance in-depth understanding of the atmospheric boundary layer structure in the inland arid desert regions of Eurasia and its developing mechanisms, thus providing an accurate scientific basis for boundary layer parameterization of the numerical model in this region.

2. Overview of the study area and climate background

The Taklamakan Desert is located in the hinterland of the Eurasian continent in the mid-latitude of the Northern Hemisphere, in the central part of the Tarim basin in Xinjiang autonomous region, China (Figure 1). It has Mount Tuomuer and Pamir Plateau to its west, Kunlun Mountains and Altun Mountains to its south, the Tianshan Mountains to its north and Lop Nur to its east. It is about 1070 km long from east to west and about 410 km wide from south to north with an area of 33.76×10^4 km^2. It is the second largest flow desert in the world, after the Rub' al Khali in Arabian Peninsula, and also a major source of sand-dust storms in China. Because the Tibetan Plateau and the surrounding mountains obstruct water vapour from other places, the Taklamakan Desert has become an extremely arid climate zone where it is dry in winter and rains less in summer. Sufficient light and heat, less precipitation, strong sunshine and great variation in temperature are climatic characteristics there. Combining such climate with sparse desert vegetation, a unique and extremely fragile natural ecosystem is formed.

The atmosphere environment observation station is in the Tazhong region (39 ° 00 ′ N, 83 ° 40 ′ E), which is the hinterland of the Taklamakan Desert with an elevation of 1099 m above mean sea level. The annual mean temperature there is 12.1 C, but the extreme maximum temperature can reach 40.0–46.0 C. Annual precipitation is around 30 mm whereas the annual evaporation potentially reaches 3812.3 mm. East winds prevail in this area with average speeds of 2.3 m s^{-1}. On average, annually there are more than 30 sand-dust storm days, over 70 flying sand days and over 100 floating dust days. Moreover, such weather events

Figure 2. CFL-03 mobile boundary layer wind-profiling radar in operation in the central Taklamakan Desert.

are seen frequently through the whole spring and summer. The field of observation around the station is open and the ground surface is covered by flow dunes and small amounts of desert shrub plants. This area shows surface characteristics of the Taklamakan Desert.

3. Detecting equipment and data

The detection equipment used include the CFL-03 mobile wind-profiling radar (Figure 2) developed by the No. 23 Research Institute of China Aerospace Science and Industry Corporation (CASIC) and the L-band radar sounding system from NanJing DaQiao Machine Co., Ltd. With a designed detection height of 3000–5000 m, the CFL-03 wind-profiling radar belongs to the category of boundary layer wind-profiling radar, having six components including transmitter, receiver, antenna, monitoring, signal processing/control and data processing. It adopts a detection mode of five fixed beams, including one vertical beam and four tilt beams at a zenith angle of 15°. These tilt beams are distributed evenly and orthogonally in azimuth. To balance the detection height and resolution in case of low-level operation, CFL-03 runs in two modes: low and high. The low mode uses narrow pulse with height resolution of 50 m, and the high mode uses wide pulse with height resolution of 100 m. The two modes work alternately to ensure concurrent high low-level

Table 1. Technical parameters of the CFL-03 mobile boundary wind-profiling radar.

Item	Parameter	Item	High mode parameter	Low mode parameter
Radar wavelength	227 mm	Pulse width	0.66 us	0.33 us
Beam width	8°	Minimum detection altitude	600 m	50 m
Beam number	5	Noise co-efficient	2 dB	2 dB
Antenna gain	25 dB	Height resolution	100 m	50 m
Feeder loss	2 dB	Coherent accumulation number	64	100
Receiver	Digital IF	FFT points	512	256
Transmitting peak power	2.36 kW	Bandwidth	1.5 MHz	3.0 MHz

resolution and high detection height. (Table 1 presents the main technical parameters of the CFL-03 wind-profiling radar.) The L-band sounding radar is a new-generation secondary wind radar developed by Chinese scientists. It has the key characteristics of high precision, quick sampling, low peak pulse power and accurate observation data, representing the realization of digitalization and automatization of upper-air meteorological sounding. (The technical parameters for the L-band sounding radar are omitted.)

From June to August 2010, the Institute of Desert Meteorology, China Meteorological Administration (CMA), conducted a clear-sky atmospheric boundary layer detection test at the atmospheric environment observation station of the Taklamakan Desert using the mobile boundary layer wind-profiling radar. In July 2011, this Institute carried out a dense observation experiment (observing four times a day) at Minfeng in the southern margin of the desert using the L-band radar sounding system.

The data used in this paper are mainly the wind-profiling radar data (original power spectrum, signal-to-noise ratio (SNR), turbulence refractive index structure constant C_n^2, vertical velocity, Doppler velocity spectrum width, virtual temperature) and densely-collected sounding data (temperature, pressure, wind speed, wind direction and relative humidity) as well as surface net radiation and sensible heat flux data.

4. Results and analysis

4.1. Surface net radiation and sensible flux features in the summer clear sky of the Taklamakan Desert hinterland

The surface thermal factor is closely bound up to the generation, development and decline process of the atmospheric boundary layer. Net radiation is the major energy source for heating the Earth's surface and atmosphere after surface net radiation balance. The near-surface sensible heat flux reflects the energy to heat the atmosphere and support the development of convection in the net radiation. Hence, net radiation and sensible heat flux are very important physical quantities that impact the generation and development of the atmospheric boundary layer.

Figures 3(a) and (b) display the diurnal variation curves of clear-sky surface net radiation and sensible heat flux on 20 June and 3 August 2010 in the Taklamakan Desert hinterland. From the net radiation curves (Figure 3(a)) it can be seen that the daily variation trends of net radiation on 20 June and 3 August are consistent and their values are similar, which are negative during the night time but turn to positive after 0800 BT (Beijing Time; UTC + 8) and then begin to increase gradually. The maximum value appears at the high noon (1200–1500 BT) with the peak value being 520 W m^{-2}. Hereafter, the net radiation diminishes gradually and after 1900–2000 BT its value becomes negative. Seen from the sensible heat flux curves (Figure 3(b)), the night time sensible heat flux is smaller, but after 0900 BT in the morning it increases gradually to a maximum at 1500–1700 BT with the peak value being about 300 W m^{-2}. After 1700 BT, the sensible heat flux starts to decline. Based on the above analysis, both the surface net radiation and sensible heat flux of clear-sky summer days in the desert hinterland are strong, with the maximum value of sensible heat flux 2–3 h later than the maximum value of net radiation. The peak value of net radiation can rise to 520 W m^{-2} whereas the peak value of sensible heat flux is 300 W m^{-2}, both of which provide abundant energy for the development of the atmospheric boundary layer in the desert, very favourable for the ground surface to heat the atmosphere and the convective boundary layer to develop strongly.

4.2. Vertical structure of the summer clear-sky atmospheric boundary layer in the Taklamakan Desert hinterland

The atmospheric boundary layer usually is classified into the daytime convective boundary layer and the night-time stable boundary layer. The daytime convective boundary layer can be divided further into surface layer, mixing layer and entrainment zone in the vertical direction whose heights can be discriminated and determined by means of wind-profiling radar SNR and C_n^2 data (Ottersten, 1969; Ecklund *et al.*, 1988; Fairall, 1991; Kusuma *et al.*, 1991; Angevine *et al.*, 1998; White *et al.*, 1991). Wang *et al.* (2015) and Wyngaard and LeMone (1980) adopted the C_n^2 peak value to determine the height of the convective boundary layer. Angevine *et al.* (1994) adopted the SNR peak value to identify the height of the convective boundary layer and the result was very close to the radiosonde observation data in that study.

Figures 4 and 5 show the time–height charts of C_n^2, SNR, vertical velocity and velocity spectral width, which were detected by wind-profiling radar on 20 June and 3 August 2010 (respectively) in the Taklamakan Desert hinterland. It can be seen from the C_n^2 time–height chart (Figure 4(a)) for 20 June that the night-time C_n^2 is smaller with the value changing within the range of $10^{-15.0}$–$10^{-17.0}$ m$^{-2/3}$. After sunrise in the morning, C_n^2 increases gradually, showing the varying trend of parabolic rise. During the period 1700–1900 BT C_n^2 becomes the strongest, its largest value domain distributes in the range of $10^{-13.0}$–$10^{-14.5}$ m$^{-2/3}$ and its height reaches about 4300 m. After 2000 BT, C_n^2 decreases. Actually, the C_n^2 time–height chart can clearly reflect the developing and evolving process of atmospheric boundary layer in desert. Using Wyngaard's approach of determining convective boundary layers (Wyngaard and LeMone, 1980), the height of the convective boundary layer can be easily discerned. In Figure 4(a), below the C_n^2 big-value zone is the height range where the mixing layer exists. The C_n^2 big-value zone mainly stands for the entrainment layer which is averagely about 500 m thick. Due to the strong entrainment and mixing action, the horizontal and

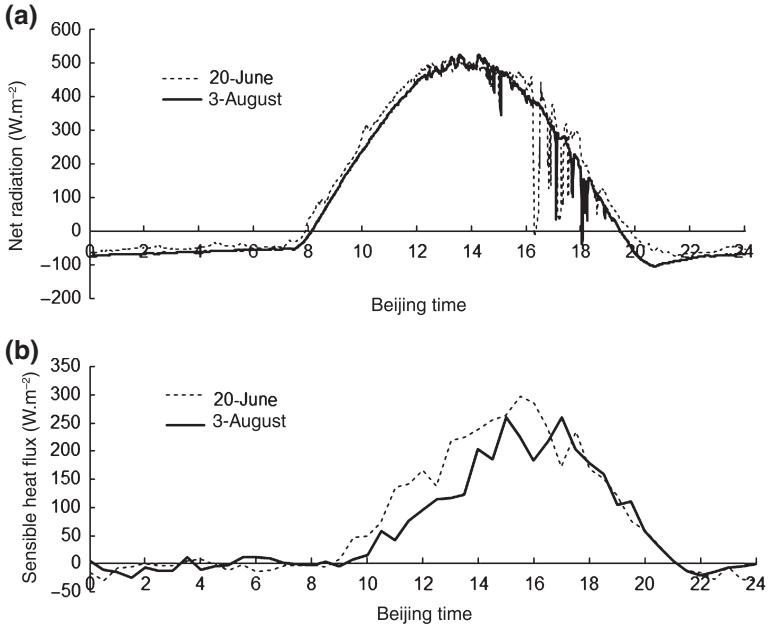

Figure 3. Daily variation curves of surface net radiation and sensible heat flux in the Taklamakan Desert hinterland on 20 June and 3 August 2010.

vertical gradients of temperature and humidity in the entrainment layer become very large, resulting in strong backscattering to radar electromagnetic waves, and formation of a bigger peak value of C_n^2. Also from Figure 4(a) it can be seen that the convective boundary layer over the Taklamakan Desert hinterland performs most energetically from 1700 to 1900 BT on 20 June, and even reaches a maximal height of 3500–4300 m. Figure 4(b) is the SNR time–height chart from 20 June. From the Figure it can be seen that the convective boundary layer starts to develop gradually from around 1000 BT and the reflected features of the mixing and entrainment layers are relatively consistent with Figure 4(a). Figure 4(c) is the time–height chart of the atmospheric vertical velocity on 20 June. It is very clear that, during the period of 1200–2000 BT when the convective boundary layer develops sufficiently, significant rising and sinking motions exist in the mixing layer below the entrainment layer and, moreover, the sinking motion plays a dominant role (positive values represent sinking motions, negative values represent rising motions). In general this is because, when thermal turbulence in the mixing layer develops towards the upper atmosphere, it is resisted severely by a temperature inversion lid at the top of the convective boundary layer and has to stop ascending. The action of gravity causes the turbulence to descend. In addition, the strong entrainment and mixing action of the entrainment layer would draw part of free atmosphere into the mixing layer, creating air sinking motion. Figure 4(d) gives out the time–height chart of the velocity spectrum width on 20 June. It reflects mainly the diversification and intensity of the turbulence motion inside the mixing layer. It can be seen from the figure that during the full development stage of the convective boundary layer the Doppler velocity spectrum is much wider, which indicates that boundary layer turbulence acts vigorously and intensely.

Figures 5(a)–(d) show the time–height chart of C_n^2, SNR, vertical velocity and velocity spectrum width from 3 to 4 August 2010. These figures show how the convective boundary layer became fully developed during 1200–2000 BT on 3 August. The evolution and height ranges of the mixing and entrainment layers can be discriminated out of the time–height chart of C_n^2 and SNR. During 1700–2000 BT the maximum height of convective boundary layer can rise to 3700 m. The average thickness of the entrainment layer is about 500 m. Within the mixing layer, there is a remarkable descending motion and larger velocity spectrum width too. Figure 5(a) reveals that, on 3 August, the deep convective boundary layer began to decline after sunset, and turned into a residual layer at night, which persisted until 1900 BT on 4 August. This process provided a favourable thermal environment for the development of the convective boundary layer on 4 August.

The above analysis suggests that the summer clear-sky convective boundary layer is extremely thick in the Taklamakan Desert hinterland and its maximum thickness can reach 4000 m, far beyond the classical height range of 1000–2000 m for boundary layers. In addition, the convective boundary layer top has significant characteristics of an entrainment layer structure with average thickness about 500 m. The strong entrainment and mixing effect can draw part of the free atmosphere into the mixing layer, forming strong descending movement of air.

Figures 6(a)–(d) are the zonal vertical profiles of potential temperatures of the desert hinterland on 20 June and 3 August 2010, which are calculated by using the NCEP reanalysis data ($1^\circ \times 1^\circ$). All of these profiles reveal that remarkable mixing layer features exist in the 900–600 hPa height with smaller potential temperature vertical gradients. The top of the mixing layer can reach about 600 hPa, which is around 3300 m high from the ground surface. This means that the summer clear-sky convective boundary layer in this desert can exceed the 3000 m height during its full development stage. Figure 7 shows the height contour map of the boundary layer over the desert area on 20 June, which is drawn based on the NCEP reanalysis data. At 1400 BT the boundary layer over the desert hinterland is at the height of approximately 3500 m, obviously higher than the height detected by the wind-profiling radar, but at 2000 BT, the boundary layer is about 3400 m high, which essentially conforms to the detection result by wind-profiling radar. So, by using NCEP reanalysis data to analyse the atmospheric boundary layer in the Taklamakan Desert, it can be further illustrated that the summer clear-sky boundary layer can develop thicker and much higher than 1000–2000 m.

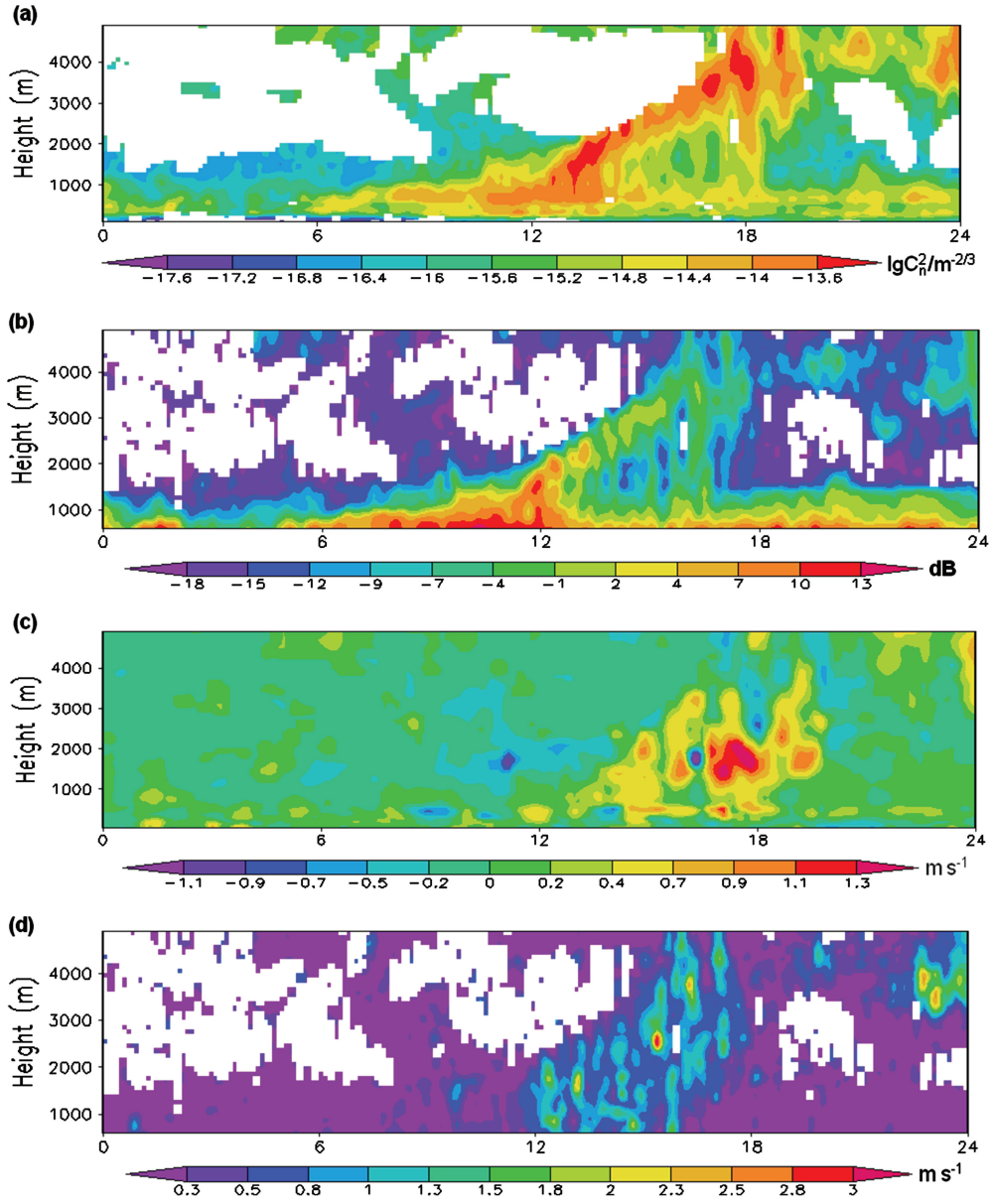

Figure 4. The time–height chart of (a) the turbulence refractive index structure constant (C_n^2), (b) the signal-to-noise ratio (SNR), (c) the vertical velocity and (d) the velocity spectrum width in Taklamakan Desert hinterland on 20 June 2010.

Figure 8 is the night time virtual temperature profiles of the desert hinterland obtained using the RASS system on 3 August and 20 June 2010. In Figure 8(a), there is an obvious temperature inversion phenomenon in the near-surface boundary layer during the night from 0000 to 0500 BT on 3 August. The temperature inversion layer is about 150 m high at 0000 BT, rising to 250 m at 0100 BT and 300 m at 0300 BT. Thereafter, it begins to descend. In addition, from the night time atmospheric virtual temperature data for 20 June (Figure 8(b)) the temperature inversion is evident also with an upper height of the temperature inversion layer of 400 m. Figure 9 presents the height contour distribution of the boundary layer at 0200 BT 3 August and 20 June on the basis of the NCEP reanalysis data. It shows that the height of the stable boundary layer at night in the desert hinterland varies within the range of 200–400 m, which corroborates with the detection result of the RASS system. In summary, the above analysis denotes that the summer clear-sky stable boundary layer at night in the Taklamakan Desert hinterland is lower in height, changing mainly in the 400 m range of the near-surface boundary layer. Combining the wind-profiling radar C_n^2 and SNR data, a general height range of the residual layer at night of 400–3500 m can be deduced roughly.

4.3. Vertical structure of the summer clear-sky boundary layer over the southern margin of the Taklamakan Desert

In order to further understand and verify the vertical structure features of the summer clear-sky atmospheric boundary layer in the Taklamakan Desert, a dense observation (four times a day at 0200, 0800, 1400 and 2000 BT) experiment was carried out at the Minfeng sounding station in the southern margin of the desert in July 2011. The potential temperature and specific humidity under the typical clear sky of 14 July 2011 are presented in Figure 10. Because thermal elements play a more important role in the arid desert boundary layer process, the potential temperature method is used in this paper to determine the height of boundary layer

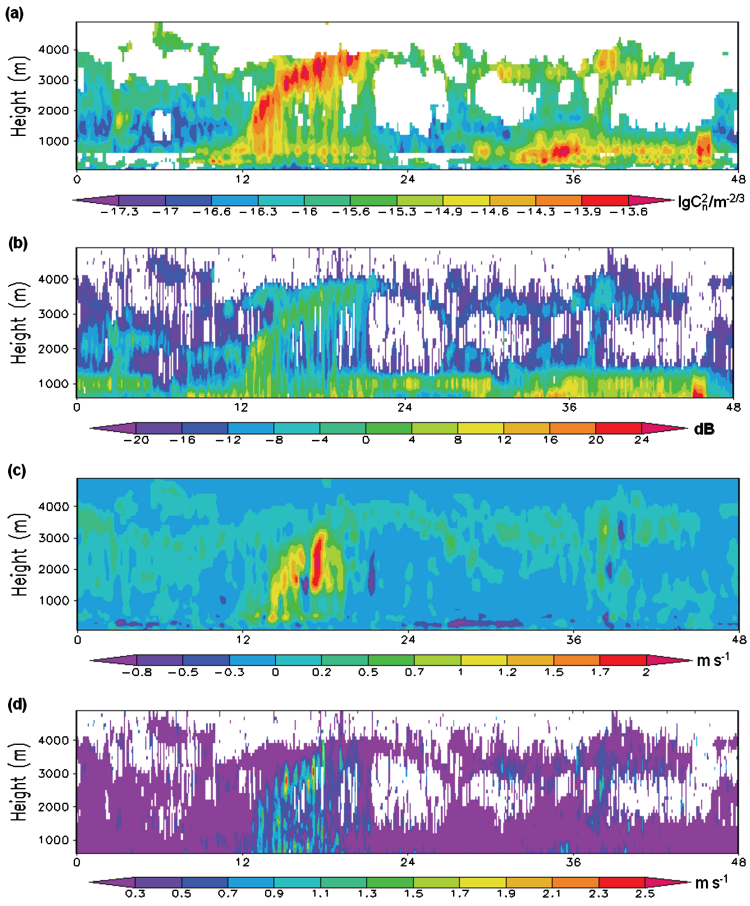

Figure 5. The time–height chart of (a) the turbulence refractive index structure constant (C_n^2), (b) the signal-to-noise ratio (SNR), (c) the vertical velocity and (d) the velocity spectrum width in the Taklamakan Desert hinterland on 3–4 August 2010.

(Seibert *et al.*, 2000; Hyun *et al.*, 2005; Qiao, 2009). Briefly, this involves taking the inverse potential temperature base of the obvious potential temperature jump or fold line as the convective mixing layer height during the daytime observations at 1400–2000 BT; that is, taking the thickness of potential temperature and specific humidity which almost does not change with height as the maximum height of convective mixing layer. During the night time (0200–0800 BT), the near-surface inverse potential temperature top is taken as the height of the stable boundary layer.

From the potential temperature profile (Figure 10(a)) the potential temperatures at 0200 and 0800 BT (before dawn) show a similar variation during which there exists an inverse potential temperature layer in the low atmosphere. At 0200 BT the height of the inverse potential temperature layer is about 400 m and by 0800 BT it has risen to the height of 600 m. Actually, the inverse potential temperature layer starts developing upward from ground at dusk and gets to its thickest before dawn. So, this inverse potential temperature layer is exactly the height of the night-time stable boundary layer. At 0200 BT the night time residual mixing layer stays in the 400–4300 m height and by 0800 BT the residual mixing layer is beween the heights of 600 and 4000 m. The air above the residual layer is free atmosphere. At noon, 1400 BT, the potential temperature profile decreases with the rising height in the low level below 250 m, which is the super diminishing adiabatic layer. In the height range of 250–3600 m the potential temperature essentially remains intact. This is the mixing layer, above which there exists an inverse potential temperature layer about 600 m thick, which is the entrainment layer. This layer is the uppermost bound of the atmospheric thermal boundary layer, above which is free atmosphere. At 2000 BT, the potential temperature profile in the low level below 150 m increased progressively with rising height, indicating that the stable boundary layer was beginning to form and develop. In the height range of 150–4100 m the mixing layer stays and above it there is the entrainment layer about 500 m thick. The free atmosphere is above the entrainment layer. Figure 10(b) is the specific humidity profile at Minfeng station on 14 July 2011. It can be seen from the figure that under the condition of a stable boundary layer overnight (0200 and 0800 BT) the specific humidity diminishes rapidly upward from the ground surface, and after getting to the top of the stable boundary layer its variation slows down. Inside the residual layer the variation in the specific humidity gradient is smaller, but in the inverse potential temperature top cover layer of the residual layer the specific humidity diminishes abruptly, so after coming out of the inverse potential temperature top cover layer the specific humidity becomes very small. Under the condition of the daytime convective boundary layer (1400 and 2000 BT), the specific humidity of the atmosphere also diminishes upward starting from the ground, but more slowly than at night. The vertical gradient of specific humidity in the mixing layer is smaller whereas the specific humidity in the entrainment layer diminishes very quickly.

In short, the above comprehensive analysis on the summer clear-sky potential temperature and specific humidity profiles of the southern margin of the Taklamakan Desert indicates that the vertical features of potential temperature and specific humidity profiles support and verify each other, both presenting consistently the typical structure features of clear-sky atmospheric

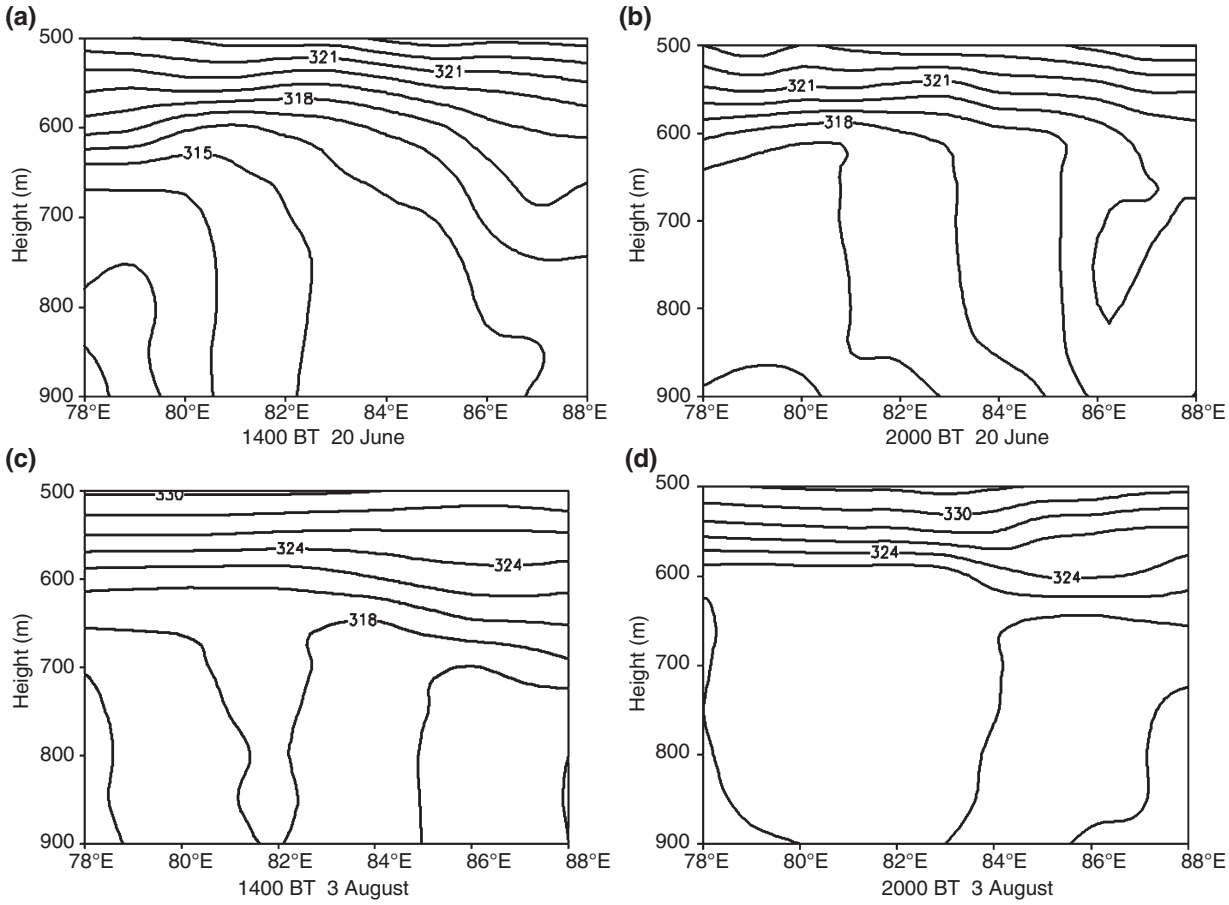

Figure 6. Zonal vertical cross-sections of potential temperature along the latitude (39°N) of the Taklamakan Desert hinterland on 20 June and 3 August 2010.

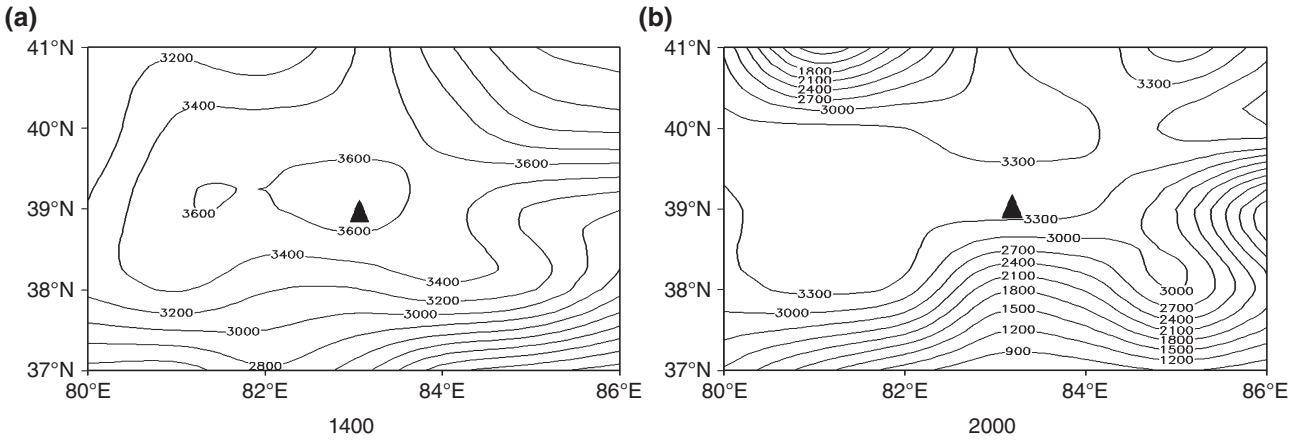

Figure 7. Height contour distribution of the atmospheric boundary layer in the Taklamakan Desert on 20 June 2010 (the black triangle represents the Taklamakan Desert Atmospheric Environment Observation Experimental Station location).

boundary layer in this region. The summer clear-sky convective boundary layer over the southern margin of the desert develops deeply and thickly in an extreme way and its maximum height can pass over 4000 m. During the night the stable boundary layer is about in the height of 400–600 m. This finding is almost the same as the research result of the clear-sky boundary layer in the desert hinterland. So according to the analysis, the detection accuracy of wind-profiling radar to the clear-sky boundary layer of the desert hinterland is verified further.

4.4. Thickness comparison of boundary layers of the Taklamakan Desert, the Tibetan Plateau and the Dunhuang region

The Taklamakan Desert lies in the arid region of Northwest China, to the north of the wide topography of the Tibetan Plateau. To find out the dominant elements that restrict and impact the evolvement of the atmospheric boundary layer in this region, the research result of this paper is compared with the research

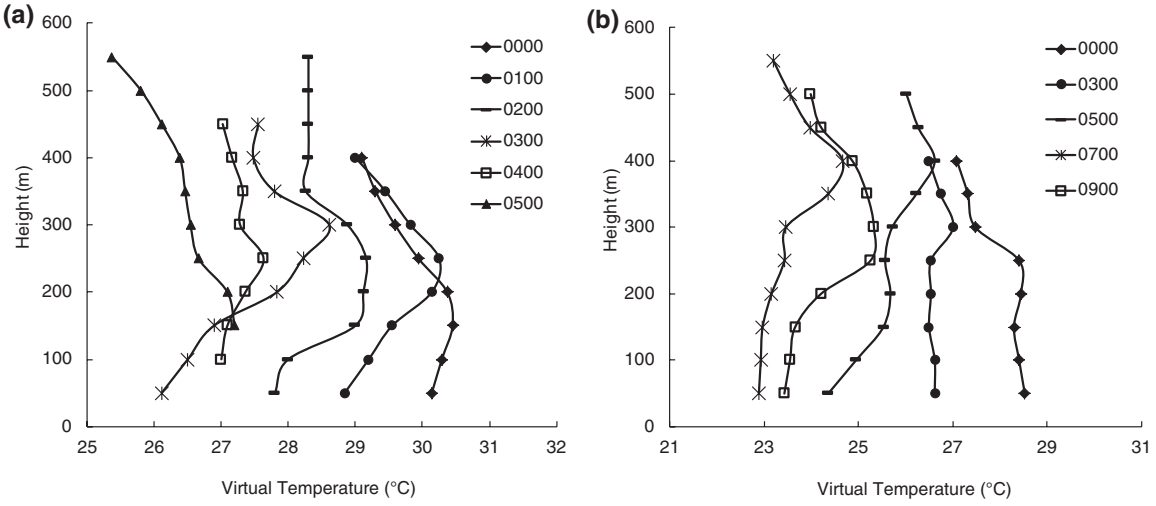

Figure 8. Atmospheric virtual temperature profiles for the nights of (a) 3 August and (b) 20 June 2010 in the Taklamakan Desert hinterland .

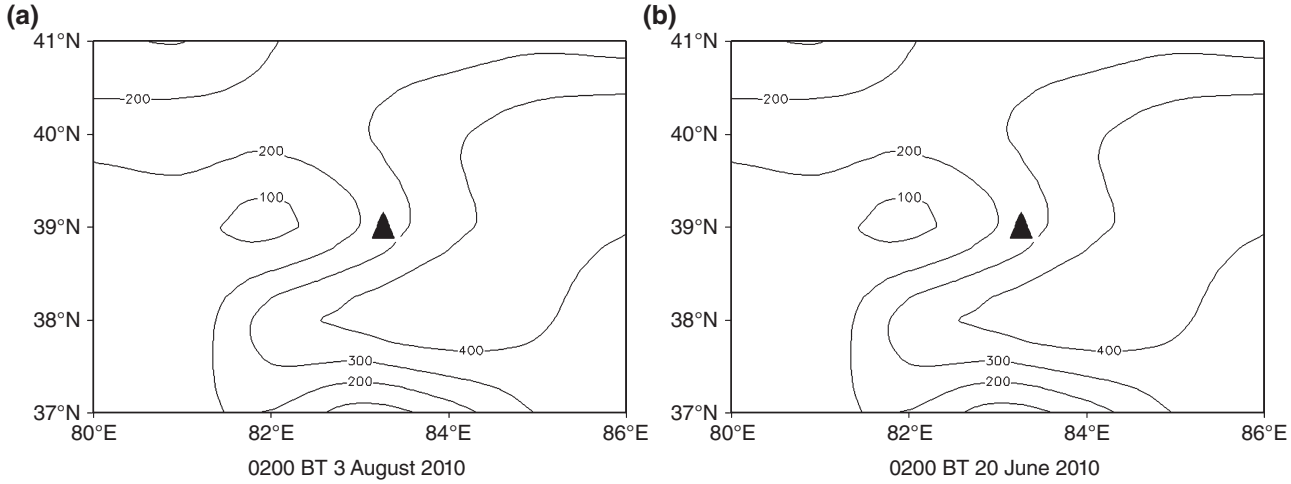

Figure 9. Height distribution of the night-time boundary layer in the Taklamakan Desert hinterland at 0200 BT 3 August and 20 June 2010.

results for the Tibetan Plateau and the Dunhuang region in the arid area of Northwest China. Ye and Gao (1979) pointed out in their study that the height of the boundary layer in the Tibetan Plateau is between 2000 and 3000 m. Xu *et al.* (2001) revealed that the summer boundary layer in the Dangxiong region of the Tibetan Plateau moves in the height range of 1850–2750 m. Wang and Ma (2008) found that the summer boundary layer in the Everest region of the Tibetan Plateau is about 1630 m at most. Zhang and Wang (2008) found *via* their research in the Dunhuang region that, on clear days in summer, the thickness of the convective boundary layer in the daytime in Dunhuang can exceed the 4000 m height and the maximum thickness of the night time stable boundary layer can reach a height of 1750 m. Based on the analysis in this paper, the maximum thickness of summer clear-sky convective boundary layers in the hinterland and southern margin of the Taklamakan Desert can reach a height of 4000 m while the night time stable boundary layer is about 400–600 m high. Thus, the characteristics of the summer clear-sky boundary layer in the Taklamakan Desert are more similar to those of Dunhuang, but very different from those of the Tibetan Plateau, indicating that the atmospheric boundary layer over the desert is dominantly restricted and affected by the underlying surface thermal action in arid regions. The research result of this paper has further verified the conclusion by Zhang *et al.* (2007) that there is an extremely thick atmospheric boundary layer in the Northwest arid region of China under clear skies in summer.

5. Conclusions

In this study, a CFL-03 boundary layer wind-profiling radar and an L-band radar sounding system, were used in a detection experiment of the atmospheric boundary layer in summer clear skies in the central part and southern margin of the Taklamakan Desert. The vertical structure characteristics of the clear-sky boundary layer and the night time stable boundary layer in the hinterland and southern margin of the desert were analysed, and the result compared with the boundary layer features in the Tibetan Plateau and the Dunhuang region. The conclusions are as follows.

1. The ground surface net radiation and sensible heat flux in summer clear sky in the hinterland of the Taklamakan Desert are strong and the peak values for net radiation can reach 520 W m^{-2} and sensible heat flux can reach 300 W m^{-2}. The strong surface thermal process provides an abundant energy

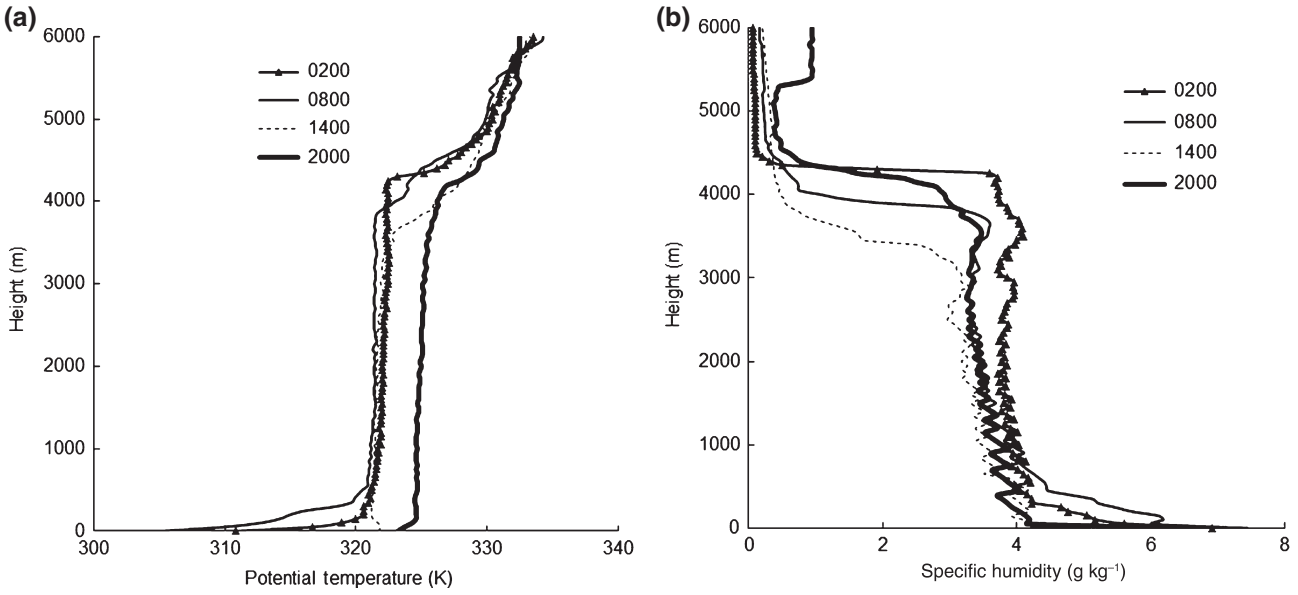

Figure 10. Clear-sky potential temperature and specific humidity profiles at Minfeng station in the southern margin of the Taklamakan Desert on 14 July 2011.

source for the development of the atmospheric boundary layer of the desert.

2. The summer clear-sky convective boundary layers in the hinterland and southern margin of the desert can develop deeply and thickly. The mixing layer can reach a thickness of 3700 m at most, above which a significant entrainment layer exists with average thickness about 500 m. The maximum thickness of the convective boundary layer can exceed 4000 m.
3. A remarkable temperature inversion phenomenon is found to exist over the summer clear-sky nights in the hinterland and southern margin of the desert. The thickness of the night time stable boundary layer is about 400–600 m, but the residual layer above it reaches a thickness of more than 3000 m generally. The deep and thick convective boundary layer is the prerequisite for the maintenance of the deep and thick residual layer at night, and, in return, the thick night time residual layer offer very good thermal environmental conditions for the development of the convective boundary layer in the daytime.
4. The thickness of the summer clear-sky convective boundary layer in Taklamakan Desert found herein conforms to the result of the research on Dunhuang, but differs greatly from the thickness of the atmospheric boundary layer in the summer for the Tibetan Plateau. The structure of the atmospheric boundary layer over this desert is restricted and influenced mainly by the underlying surface thermal action in arid regions. The phenomenon of an atmospheric boundary layer with supernormal thickness under the clear sky in summer over the arid regions in Northwest China is further confirmed by this research.

Acknowledgements

This research is jointly supported by the Project of National Natural Science Foundation of China (41305035), the Project for public good dedicated to the meteorological sector in China (GYHY201406001) and the Project of National Natural Science Foundation of China (41575008). The authors thank the desert meteorology science teams. Supported data can be required from WMZ (yurenkeji@idm.cn).

References

Angevine WM, Grimsdell AW, Hartten LM, Delany AC. 1998. The flatland boundary layer experiments. *Bull. Am. Meteorol. Soc.* **79**: 419–431.

Angevine WM, White AB, Avery SK. 1994. Boundary-layer depth and entrainment zone characterization with a boundary-layer profiler. *Bound. Layer Meteorol.* **68**: 375–385.

Ecklund WL, Carter DA, Balsley BB. 1988. A UHF wind profiler for the boundary layer: brief description and initial results. *J. Atmos. Ocean. Tech.* **5**: 432–441.

Fairall CW. 1991. The humidity/temperature sensitivity of clear-Air radars for the cloudfree convective boundary layer. *J. Appl. Meteorol.* **8**: 1064–1074.

Gamo M. 1996. Thickness of the convection and large-scale subsidence above deserts. *Bound. Layer Meteorol.* **79**: 265–278.

Gamo M, Goyal P, Manju K, Kumari M, Mohanty UC, Singh MP. 1994. Mixed-layer characteristics as related to the monsoon climate of New Delhi, India. *Bound. Layer Meteorol.* **67**: 213–227.

Garratt JR. 1992. *The Atmospheric Boundary Layer*. Cambridge University Press: Cambridge; 1–3.

He Q. 2009. Observation study of atmospheric boundary layer structure and land atmosphere interaction in the Tazhong of Taklimakan Desert. Doctoral Dissertation, Nanjing University of Information Science & Technology: Nanjing, China; 80–100.

He Q, Jing LL, Yang XH, Liu XC, Li ZJ, Liu Q, et al. 2010a. Analysis on O_3 concentration and affecting factors for boundary-layer in hinterland of Taklimakan Desert in Autumn. *Plateau. Meteorol.* **29**: 214–221 (in Chinese).

He Q, Liu Q, Yang XH, Ali MMTM, Huo W, Liang Y. 2010b. Profiles of atmosphere boundary layer Ozone in winter over hinterland of Taklimakan Desert. *J. Desert Res.* **30**: 909–916 (in Chinese).

Hyun YK, Kim KE, Ha KJ. 2005. A comparison of methods to estimate the height of stable boundary layer over atemperate grassland. *Agric. Forest. Meteorol.* **132**: 132–142.

Kusuma GR, Raman S, Prahbu A. 1991. Boundary layer height over the monsoon trough region during active and break phases. *Bound. Layer Meteorol.* **57**: 29–138.

Liu YQ, He Q, Zhang HS, Ali MMTM. 2012. Improving the CoLM in Taklimakan Desert hinterland with accurate key parameters and an appropriate parameterization scheme. *Adv. Atmos. Sci.* **29**: 381–390 (in Chinese).

Marsham JH, Parker DJ, Crams CM, Johnson BT, Grey WMF, Ross AN. 2008. Observations of mesoscale and boundary-layer scale circulations affecting dust transport and uplift over the Sahara. *Atmos. Chem. Phys.* **8**: 6979–6993.

Ottersten H. 1969. Atmospheric structure and radar backscattering in clear air. *Radio Sci.* **4**: 1179–1193.

Qiao J. 2009. The temporal and spatial characteristics of atmospheric boundary layer and its formation mechanism over arid region of northwest China, Masters Dissertation, Chinese Academy of Meteorological Sciences: Beijing, China; 6–12.

Raman S, Templeman B, Templeman S, Holt T, Murthy AB, Singh MP. 1990. Structure of the Indian southwesterly pre-monsoon and monsoon boundary layers: observations and numerical simulation. *Atmos. Environ.* **24**: 723–734.

Seibert P, Beyrich F, Gryning SE, Joffre S, Rasmussen A, Tercier P. 2000. Review and intercomparison of operational methods for the determination of the mixing height. *Atmos. Environ.* **34**: 1001–1027.

Takemi T. 1999. Structure and evolution of a severe squall line over the arid region in northwest China. *Mon. Weather Rev.* **127**: 1301–1309.

Wang SZ, Ma YM. 2008. The structure of atmospheric boundary Layer over mount Qomolangma in summer. *J. Glaciol. Geocryol.* **30**: 681–687 (in Chinese).

Wang YJ, Xu XD, Zhao TL, Sun JH, Yao WQ, Zhou MY. 2015. Structures of convection and turbulent kinetic energy in boundary layer over the southeastern edge of the Tibetan Plateau. *Sci. China Earth Sci.* **58**: 1198–1209.

Wen YT, Miao QL, He Q, Li LL. 2010. Observations on turbulence intensity and turbulent kinetic energy of surface layer in spring and summer in Taklimakan hinterland. *J. Desert Res.* **30**: 439–444 (in Chinese).

White AB, Fairall CW, Thompson DW. 1991. Radar observations of humidity variability in and above the marine atmospheric boundary layer. *J. Atmos. Oceanic Technol.* **8**: 639–658.

Wyngaard JC, LeMone MA. 1980. Behavior of the refractive index structure parameter in the entraining convective boundary layer. *J. Atmos. Sci.* **37**: 1573–1585.

Xu XD, Wang YJ, Wei WS, Zhao TL, Xu HX. 2014. Summertime precipitation process and atmospheric water cycle over Tarim Basin under the specific large terrain background. *Desert Oasis Meteorol.* **8**: 1–11 (in Chinese).

Xu XD, Zhou MY, Chen JY, Bian LG, Zhang GZ, Liu HZ, et al. 2001. Integrated physical images of the dynamic and thermal structures of land-atmospheric process in Tibetan Plateau. *Sci. China Ser. D.* **31**: 428–440.

Yang XH, He Q, Ali MMTM, Huo W, Liu XC. 2013. Diurnal variations of saltation activity at Tazhong: the hinterland of Taklimakan Desert. *Meteorol. Atmos. Phys.* **119**: 177–185.

Ye DZ, Gao YX. 1979. *Meteorology of the Tibetan Plateau*. China Science Press: Beijing; 89–101.

Zhang Q. 2007. Study on depth of atmospheric thermal boundary layer in extreme arid desert regions. *J. Desert Res.* **27**: 614–620 (in Chinese).

Zhang Q, Wang S. 2008. A study on atmospheric boundary layer structure on a clear day in the arid region in northwest China. *Acta Meteorol. Sin.* **66**: 599–608 (in Chinese).

Zhang Q, Zhang J, Qiao J, Wang S. 2011. Relationship of atmospheric boundary layer depth with thermodynamic processes at the land surface in arid regions of China. *Sci. China Earth. Sci.* **41**: 1365–1374.

Zhang Q, Zhao YD, Wang S, Ma F. 2007. A study on atmospheric thermal boundary layer structure in extremely arid desert and Gobi region on the clear day in summer. *Adv. Earth Sci.* **22**: 1150–1159 (in Chinese).

